See the corresponding editorial in this issue, pp 866–870.

J Neurosurg 116:871–881, 2012

Identification of a dichotomy in morphological predictors of rupture status between sidewall- and bifurcation-type intracranial aneurysms

Clinical article

Merih I. Baharoglu, M.D., Alexandra Lauric, Ph.D., Bu-Lang Gao, M.D., Ph.D., and Adel M. Malek, M.D., Ph.D.

Cerebrovascular and Endovascular Division, Department of Neurosurgery, Tufts Medical Center and Tufts University School of Medicine, Boston, Massachusetts

Object. Prediction of aneurysm rupture likelihood is clinically valuable, given that more unruptured aneurysms are being discovered incidentally with the increased use of imaging. The authors set out to evaluate the relative performance of morphological features for rupture status discrimination in the context of the divergent geometrical and hemodynamic characteristics of sidewall- and bifurcation-type aneurysms.

Methods. Catheter 3D rotational angiographic images of 271 consecutive aneurysms (101 ruptured, 135 bifurcation type) were used to assess the following parameters in 3D: maximum diameter (D_{max}), height, height/width ratio, aspect ratio, size ratio, nonsphericity index, and inflow angle. Univariate statistics applied to the bifurcation, sidewall, and combined (bifurcation + sidewall) sets identified significant features for inclusion in multivariate analysis yielding area under the curve (AUC) and optimal thresholds in the receiver-operating characteristic. Furthermore, a computational fluid dynamics analysis was performed to evaluate the flow and wall shear stress conditions inside sidewall and bifurcation aneurysms at different inflow angles.

Results. The mean D_{max}, height, and inflow angle were significantly greater in ruptured sidewall aneurysms than in unruptured sidewall aneurysms, but showed no difference between ruptured and unruptured bifurcation lesions. There was a statistically significant difference between ruptured and unruptured aneurysms for all measured features in the combined set. Multivariate analysis identified the following: 1) nonsphericity index as the only rupture status discriminator in bifurcation lesions (AUC = 0.67); 2) height/width ratio, size ratio, and inflow angle as strong discriminators in sidewall lesions (AUC = 0.87); and 3) height/width ratio, inflow angle, and size ratio as intermediate discriminators in the combined group (AUC = 0.76). Computational fluid dynamics analysis showed that although increasing inflow angle in a sidewall model led to deeper penetration of flow, higher velocities, and higher wall shear stress inside the aneurysm dome, it produced the exact opposite results in a bifurcation model.

Conclusions. Retrospective morphological and hemodynamic analysis point to a dichotomy between sidewall and bifurcation aneurysms with respect to performance of shape and size parameters in identifying rupture status, suggesting the need for aneurysm type–based analyses in future studies. The current most commonly used clinical risk assessment metric, D_{max}, was found to be of no value in differentiating between ruptured and unruptured bifurcation aneurysms.

(http://thejns.org/doi/abs/10.3171/2011.11.JNS11311)

Key Words • **intracranial aneurysm** • **morphology** • **aneurysm type** • **subarachnoid hemorrhage** • **rupture risk** • **vascular disorders**

The detection of incidental unruptured intracranial aneurysms has increased with the advent of improved vascular imaging methods.[27] Although aneurysmal subarachnoid hemorrhage carries a mortality rate of 40%–50% and a morbidity rate of 10%–20%,[4,7,26] the management of these unruptured lesions remains controversial.[28,29] Recent studies[13,30] suggest these aneurysms have a relative low annual rupture risk of 0.1%–0.2%, in contrast to earlier data[14,15,33,36] that suggested a yearly risk closer to 1%–2%. At the same time, both surgical and endovascular preventative treatments of unruptured aneurysms carry an age-dependent risk of complication. The ISUIA study[13] revealed mortality and morbidity rates to be as high as 10%–13% following microsurgical clipping, and an aneurysm size threshold between 7–10 mm was proposed for considering aggressive therapy.[13,31]

Abbreviations used in this paper: AUC = area under the receiver-operating curve; CFD = computational fluid dynamics; D_{max} = largest diameter of aneurysm dome; ICA = internal carotid artery; ISUIA = International Study of Unruptured Intracranial Aneurysms; PCoA = posterior communicating artery; ROC = receiver-operating curve or characteristic.

This article contains some figures that are displayed in color online but in black and white in the print edition.

Brought to you by Tufts University | Unauthenticated | Downloaded 11/04/25 02:25 PM UTC

Clearly, the decision to treat unruptured aneurysms needs to be carefully balanced against the risk of rupture.

Consequently, the ability to predict the likelihood for an incidental aneurysm to proceed to rupture would be of great clinical value. Clinical rupture risk assessment has centered on the concept of maximum aneurysm size (D_{max}), which is the most studied aneurysm measure in prospective, retrospective, and clinical evaluations.[13–15,30,31] While many studies report size to be a significant feature for rupture prediction, an increasing number of analyses point to its shortcomings and clinical unreliability, as many ruptured aneurysms are small in size. The reason for the discrepancy in the clinical relevance of D_{max} has remained elusive, with selection bias and prospective versus retrospective design as possible culprits. This has encouraged the introduction of additional features based on size measurements,[12,25] location,[13,30] and shape,[19] which have demonstrated encouraging performance in discriminating between ruptured and unruptured lesions in retrospective analyses. However, the introduction of this multitude of shape parameters has also made it increasingly difficult for clinicians to assess their relative merit. This difficulty has been compounded by differences in study populations, visualization and measurement techniques (2D vs 3D), and type of acquired data (cross-sectional CT angiography[19] or MR angiography vs catheter-based digital subtraction angiography[22] and 3D rotational angiography[6]). In addition, previous studies have analyzed saccular aneurysms in a monolithic fashion without differentiation between sidewall and bifurcation types, despite evidence of important differences in aneurysm hemodynamic patterns in these subsets.[11] In a recent study[2] on the role of parent vessel inflow angle in rupture status prediction, important hemodynamic differences were noted between sidewall and bifurcation lesions, which we set out to explore further.

The object of the current study is to evaluate the performance of established morphological descriptors in assessing rupture status among intracranial saccular aneurysms using the largest high-resolution catheter-based 3D-rotational angiography data set to date, measured and analyzed in 3D space within the context of the hemodynamic and morphological divergence between sidewall and bifurcation lesions.

Methods

Patient Selection and Demographic Characteristics

Consecutive high-resolution 3D angiographic data obtained in patients with intradural intracranial aneurysms that were diagnosed and treated between November 2001 and December 2008 were reviewed for this study from a prospectively maintained database. Fusiform, mycotic, and extradural aneurysms were excluded—the last because of their known different natural history and low risk of subarachnoid hemorrhage.[17] All angiographic data within this set were obtained in emergent fashion and prior to vasospasm onset. Aneurysm status was labeled by the treating clinicians at the time of presentation. The temporal evolution of aneurysm shape and clinical symptomatology were not followed up clinically and were not available for ruptured lesions prior to their rupture.

Differentiation Between Sidewall and Bifurcation Types

Aneurysms were defined as sidewall lesions if they originated from only one parent vessel or from the origin of a branch that was much smaller than the parent vessel[18] (less than one-fifth the diameter[35]). Aneurysms were defined as bifurcation lesions if they were located at major bifurcations in the cerebral vasculature.[18] Under this classification system, aneurysms located at the ophthalmic or anterior choroidal artery bifurcations were classified as sidewall, because the bifurcating vessel is many times smaller in diameter than the ICA off which the aneurysms originated. As for aneurysms originating off the PCoA, the aneurysms were classified as sidewall except for lesions that were located at a fetal posterior artery bifurcation or where the PCoA was prominent and not merely a vestigial side branch. Posterior communicating artery aneurysms, originating at the carotid artery–posterior communication junction, were thus classified as either sidewall or bifurcation, depending on the size of the PCoA relative to the ICA diameter.

Cerebral Angiography and Morphological Feature Extraction

Three-dimensional catheter-based cerebral angiograms were obtained using either a Philips Integris or Siemens Artis calibrated biplane system, with volume reconstruction using their respective clinical software packages, to yield a 3D volumetric data set. The 3D data sets included the aneurysm and its parent vessel (Fig. 1A–C). The image processing of the 3D data sets (including segmentation, surface creation, and 3D measurement) was performed in Amira Version 5.1 (Visage Imaging).

The following aneurysm characteristics were extracted in 3D space as previously described (Fig. 1D):[2] maximum dome diameter (D_{max}), aneurysm height and width, neck width, inflow angle, and parent and daughter vessel diameters (D_1, D_2, D_3). The parent vessel diameter and aneurysm neck were measured in 3D space using a cross-sectional plane and assuming an elliptical contour with major and minor axes that were averaged. In addition, the height/width ratio (height divided by width), aspect ratio[24] (height divided by neck width), and size ratio[6] (height divided by the average parent vessel diameter) were calculated. Finally, the nonsphericity index, ranging from 0 (perfect sphere) to 1, was calculated for each aneurysm using the formula introduced by Raghavan et al.[20]

Computational Fluid Dynamics Analysis

Aneurysm models were constructed with SolidWorks software (Dassault Systèmes SolidWorks Corp.). The 2 sidewall aneurysm models measured 8 × 4 mm off a 4-mm-diameter vessel, with one model having a low inflow angle (50°) and the other a high inflow angle (140°). The bifurcation model was constructed using the same parent vessel dimensions, and the same neck connector was shared by both angular configurations. In one bifurcation model the aneurysm dome was in line with the par-

Brought to you by Tufts University | Unauthenticated | Downloaded 11/04/25 02:25 PM UTC

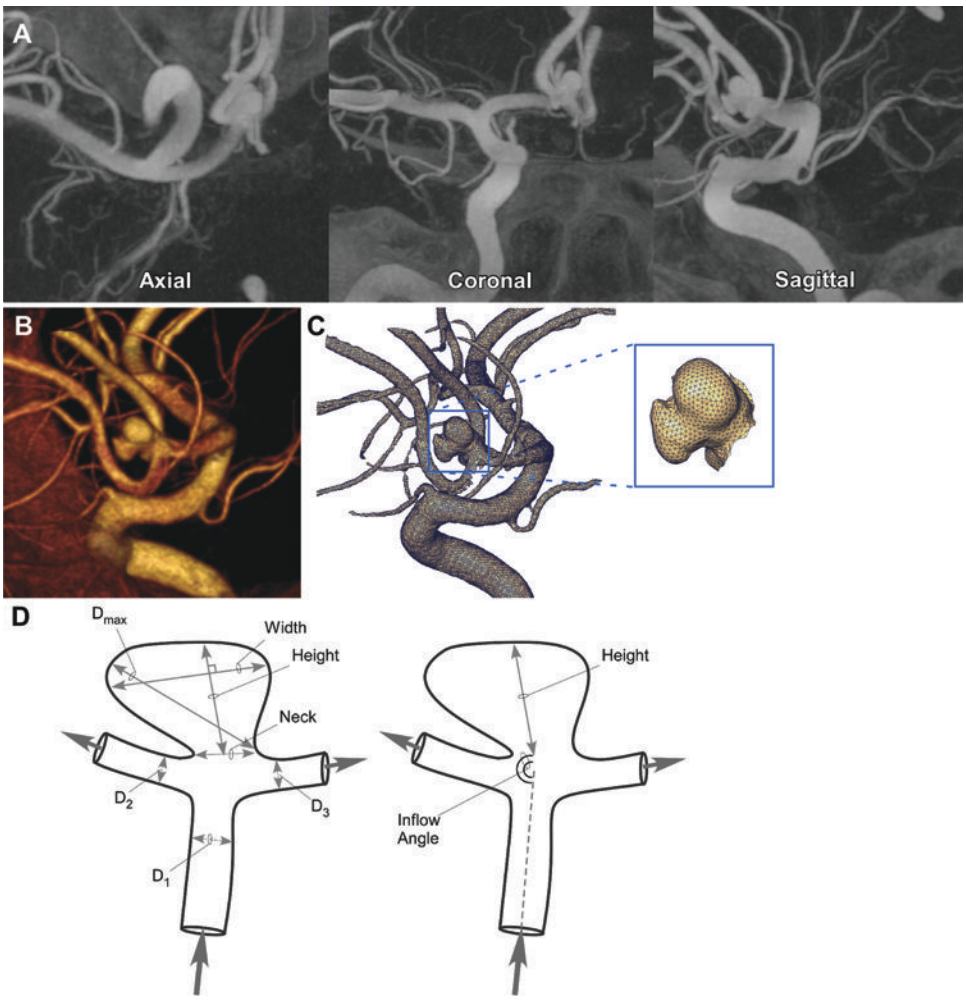


Fig. 1. Segmentation and isolation of aneurysms using catheter-based high-resolution 3D rotational angiography. **A:** Maximum-intensity projection of the reconstructed 3D volumetric data set in axial, coronal, and sagittal views showing a ruptured anterior communicating artery aneurysm. **B–D:** Volumetric renderings and schematic cross-sections. The 3D volumetric rendering **(B)** enables segmentation of the vascular structure from surrounding tissue and representation of the vessel surface as a triangular mesh **(C)**, which in turn enables separation of the aneurysm dome for surface/volume analysis and feature measurement in 3D space, as shown in schematic cross-sectional fashion for a bifurcation-type aneurysm **(D)**.

ent vessel, thus producing a high inflow angle (180°). The other model had a low inflow angle (110°) in one plane and was orthogonal to the parent and daughter vessels in the other plane. The daughter vessels were symmetrical and at a 120° angle with a radius of 1.587 mm, which was determined according to the principle of optimality to maintain constant wall shear stress magnitude at the bifurcation.[10] The neck was approximately 5 diameters downstream from the inflow, enabling fully developed flow.[34] The parametric design included a spherical neck connector, which resulted in the same neck and aneurysm dimensions for both models.[2] Thus, the inflow angle was the only variable to change.

High-resolution polyhedral meshes with prismatic boundary layer enrichment were generated with Star-CCM Version 4.02 (CD-adapco) at a count of approximately 1×10^6 cells. Fluent Version 6.3.26 (Ansys) was used to perform the finite-volume solution in the laminar double-precision unsteady regimen as previously described.[2] Postprocessing was performed in EnSight Version 9 (Computational Engineering International, Inc.). Cut planes were obtained at the center of the vessel and used to visualize velocity magnitude and vectorial distribution. Wall shear stress was visualized on the surface of the aneurysm dome and was also computed for the upper half portion of the dome in line with the parent vessel's main axis. The values along this cutline were analyzed along the distance marched for distribution and mean ± standard deviation.

Statistical Analysis

The data were analyzed using JMP Version 8.02 (SAS Institute). Statistical significance was assumed at $p < 0.05$. The analysis was performed retrospectively, and the aneurysms were divided into ruptured and unruptured subsets for analysis. All variables were tested independently using the Student t-test. The analysis was performed on the sidewall and bifurcation subsets, as well as the overall

Brought to you by Tufts University | Unauthenticated | Downloaded 11/04/25 02:25 PM UTC

combined group. An additional univariate analysis was performed within the PCoA aneurysm group because PCoA aneurysms were labeled as either sidewall or bifurcation lesions depending on the size of the PCoA.

Multivariate logistic regression was performed separately, using forward stepwise regression to control for those morphological features that achieved univariate statistical significance with $p < 0.05$. Receiver-operating characteristics analysis was used to determine sensitivity and specificity by use of AUC. A separate multivariate analysis was performed to assess the disparate value of the sidewall/bifurcation subtype as a dichotomous variable in the overall combined group. Furthermore, the value of the interaction variables of the sidewall/bifurcation subtype with the other aneurysm morphological variables was assessed again with a stepwise logistic regression model to address the issue of independence.

Results

Demographics and Presentation

Data on a total of 271 aneurysms in 229 patients were available for analysis. Of these aneurysms, 135 (49.8%) were classified as bifurcation and 136 (50.2%) as sidewall. The distribution of locations is shown in Table 1. The patients' mean age was 56 years (range 11–92 years) and 169 (73.8%) were women. A total of 101 (37.3%) of the 271 aneurysms (34 in the sidewall group [25.0%] and 67 in the bifurcation group [49.6%]) had ruptured.

Aneurysm Morphological Univariate Analysis

The results for the entire data set are summarized in Table 2, presented for the sidewall, bifurcation, and combined (sidewall + bifurcation) sets. The D_{max} was not found to differentiate between ruptured (6.96 mm, 95% CI 6.23–7.68 mm) and unruptured (6.79 mm, 95% CI 6.07–7.51 mm) bifurcation aneurysms ($p = 0.74$, AUC = 0.51) (Table 2). In contrast, D_{max} was significantly greater in ruptured sidewall aneurysms (9.33 mm, 95% CI 8.20–10.45 mm vs 6.22, 95% CI 5.56–6.88 mm) ($p < 0.001$, AUC = 0.75) (Fig. 2). Similarly, inflow angle within the bifurcation aneurysm subset was almost identical in ruptured (134.3°, 95% CI 127.9°–140.7°) and unruptured (132.2°, 95% CI 125.8°–138.5°) lesions ($p = 0.64$, AUC = 0.53), whereas in sidewall aneurysms, inflow angle was greater in ruptured lesions (125.1°, 95% CI 117.9°–132.4° vs 107.2°, 95% CI 103.1°–111.4°) ($p < 0.001$, AUC = 0.71). Following the same trend, height, height/width ratio, and size ratio did not differentiate between ruptured and unruptured bifurcation aneurysms, but were all significantly greater in ruptured sidewall compared with unruptured sidewall lesions. The nonsphericity index and aspect ratio were the only 2 parameters found to differentiate between ruptured and unruptured aneurysms within both the sidewall and the bifurcation groups.

Within the bifurcation group, only 2 parameters achieved statistical significance, both with marginal AUC performance: nonsphericity index (AUC = 0.67) and aspect ratio (AUC = 0.64). The univariate predictive power was uniformly greater in sidewall compared with bifurcation aneurysms for the descriptors evaluated herein. In the combined group (bifurcation + sidewall), all evaluated features achieved statistical significance on univariate analysis, although overall performance was poorer than in the sidewall group.

TABLE 1: Distribution of 271 aneurysms by location*

Location	No. of Aneurysms (%)	Mean D_{max}	SW	BIF
ACoA	58 (21.4)	6.50 ± 2.72		58
ICA	52 (19.2)	6.52 ± 3.90	52	
PCoA	49 (18.1)	8.04 ± 3.49	39	10
MCA	40 (14.8)	6.92 ± 3.41		40
BA	12 (4.4)	8.05 ± 2.81		12
OphA	24 (8.9)	7.17 ± 3.20	24	
ICAB	10 (3.7)	6.61 ± 2.30		10
AChA	10 (3.7)	4.77 ± 2.20	10	
SCA	3 (1.1)	4.30 ± 2.25		3
ACA	5 (1.8)	7.61 ± 4.99	5	
VA	4 (1.5)	6.48 ± 1.38	4	
PICA	2 (0.7)	7.00 ± 1.65		2
PCA	2 (0.7)	9.37 ± 1.78	2	

* ACA = anterior cerebral artery; AChA = anterior choroidal artery; ACoA = anterior communicating artery; BA = basilar artery; BIF = bifurcation; ICAB = internal carotid artery bifurcation; MCA = middle cerebral artery; OphA = ophthalmic artery; PCA = posterior cerebral artery; PICA = posterior inferior cerebellar artery; SCA = superior cerebellar artery; SW = sidewall; VA = vertebral artery.

To evaluate the effect of aneurysm type (sidewall vs bifurcation) independent of aneurysm location, we closely examined the PCoA subset, because aneurysms at that location can be classified as either sidewall or bifurcation type depending on the relative caliber of the PCoA. Analysis of the 49 PCoA aneurysms showed that D_{max} differed significantly between ruptured and unruptured aneurysms in the sidewall PCoA subset ($p = 0.003$), but was not relevant as a rupture status discriminator in the bifurcation PCoA subset ($p = 0.72$). Similarly, height, height/width ratio, and size ratio showed no statistically significant difference between ruptured and unruptured aneurysms in the bifurcation PCoA group but did show a statistically significant difference in the sidewall PCoA group. Aspect ratio was the only size parameter in the bifurcation PCoA group that showed a statistically significant difference between ruptured and unruptured aneurysms.

Multivariate Analysis

Within the bifurcation group, aspect ratio and nonsphericity index were included in the logistic model. Nonsphericity index alone was identified as independently significant, though with a marginal AUC of 0.67. In the sidewall group D_{max}, height, aspect ratio, height/width ratio, size ratio, inflow angle, and nonsphericity index were included in the logistic model. Height/width ratio, size ratio, and inflow angle were the features identified as strong

Brought to you by Tufts University | Unauthenticated | Downloaded 11/04/25 02:25 PM UTC

TABLE 2: Results from univariate analysis for morphological parameters examined*

Group & Feature	Ruptured		Unruptured		p Value	AUC
	Mean	95% CI	Mean	95% CI		
BIF						
D_{max} (mm)	6.96	6.23–7.68	6.79	6.07–7.51	0.74	0.51
H (mm)	6.08	5.38–6.78	5.62	4.93–6.32	0.36	0.55
AR	1.79	1.62–1.98	1.44	1.25–1.61	0.008†	0.64
H/W	1.39	1.28–1.51	1.26	1.15–1.37	0.11	0.62
SR	3.09	2.69–3.50	2.59	2.19–3.00	0.09	0.59
IA (°)	134.3	127.9–140.7	132.2	125.8–138.5	0.64	0.53
NSI	0.25	0.23–0.27	0.20	0.18–0.22	0.001†	0.67
SW						
D_{max} (mm)	9.33	8.20–10.5	6.22	5.56–6.88	<0.001†	0.75
H (mm)	8.75	7.69–9.80	5.04	4.43–5.64	<0.001†	0.81
AR	2.10	1.85–2.35	1.36	1.22–1.51	<0.001†	0.77
H/W	1.62	1.47–1.77	1.08	0.99–1.16	<0.001†	0.78
SR	2.86	2.48–3.23	1.48	1.26–1.70	<0.001†	0.82
IA (°)	125.1	117.9–132.4	107.2	103.1–111.4	<0.001†	0.71
NSI	0.26	0.23–0.30	0.20	0.18–0.22	0.008†	0.71
combined						
D_{max}	7.76	7.12–8.39	6.45	5.96–6.94	0.002†	0.61
H (mm)	6.98	6.37–7.58	5.27	4.80–5.74	<0.001†	0.65
AR	1.89	1.75–2.04	1.39	1.28–1.51	<0.001†	0.70
H/W	1.47	1.38–1.56	1.15	1.08–1.22	<0.001†	0.71
SR	3.01	2.72–3.30	1.92	1.70–2.15	<0.001†	0.73
IA (°)	131.3	126.2–136.4	117.2	113.3–121.1	<0.001†	0.66
NSI	0.25	0.23–0.27	0.20	0.19–0.22	<0.001†	0.69

* AR = aspect ratio; H = height of aneurysm dome; H/W = height/width ratio; IA = inflow angle; NSI = nonsphericity index; SR = size ratio.

† Statistically significant.

predictors for rupture status with an excellent AUC of 0.87 (Table 3). The height/width ratio seemed to perform best, with an odds ratio of 7.97.

In the combined group (bifurcation + sidewall) all studied parameters were included in the logistic model. Height/width ratio, size ratio, and inflow angle were again the only features identified as independently significant, though with an intermediate performance with an AUC of 0.76 (Fig. 3). The ROC curves corresponding to the logistic regression models for sidewall and bifurcation groups were compared using their AUC and standard error values and were found to have statistically significantly different discriminant capabilities for aneurysm rupture status ($p = 0.012$), with the sidewall model having better results.

In a separate analysis, the sidewall/bifurcation label was added as a separate dichotomous variable to evaluate its interaction effect with the size- and shape-based parameters presented in this work. We found that interaction parameters based on D_{max}, height, height/width ratio, inflow angle, and size ratio were significant in discriminating ruptured status in the combined group (sidewall + bifurcation). As expected, interaction parameters based on aspect ratio and nonsphericity index, which were the only parameters significant in both the bifurcation and the sidewall groups, were not statistically significant in the combined group.

Hemodynamic Differences in Sidewall and Bifurcation Aneurysms

In light of the contrasting dependence of rupture status on shape parameters, a CFD analysis was carried out. We set out to search for any fundamental flow pattern differences between bifurcation- and sidewall-type aneurysms (Fig. 4A). As previously described,[2] increasing inflow angle in a sidewall model resulted in deeper penetration of flow into the aneurysm dome with consequent higher velocities near the tip of the dome (Fig. 4B, bottom). In contrast, increasing inflow angle in a bifurcation model resulted in reduction of brisk flow in the dome (Fig. 4B, top) to near complete stagnation with secondary flow limited to the sides of the aneurysm dome near its neck. The velocities in the bifurcation models were also higher throughout than those in the sidewall models in this analysis. Analysis of the wall shear stress distribution revealed much lower wall shear stress values in the high

Brought to you by Tufts University | Unauthenticated | Downloaded 11/04/25 02:25 PM UTC

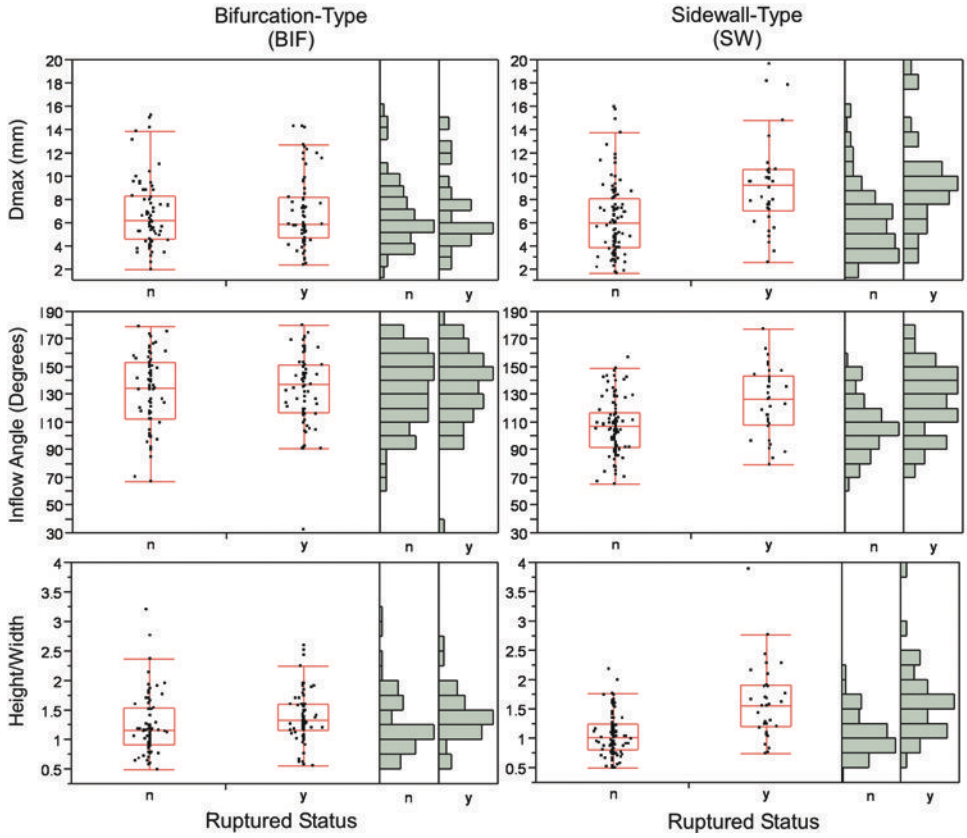


Fig. 2. Box and whisker plots showing distribution of size (D_{max}), inflow angle, and height/width ratio for ruptured (y) and unruptured (n) aneurysms analyzed separately for bifurcation and sidewall types.

inflow-angle bifurcation model than in its lower inflow-angle counterpart; this is in direct contrast to higher wall shear stress in sidewall aneurysms with higher inflow angle (Fig. 4C).[3] Quantitative sampling of the wall shear stress along a sagittal line in the upper half of the aneurysm dome in all 4 models revealed higher wall shear stress values in the bifurcation models than in their sidewall counterparts and also again showed the opposite effects of increasing inflow angle between bifurcation and sidewall configurations. The mean values of wall shear stress on the upper half of the dome decreased from 5.6 ± 0.36 dyne/cm^2 in the low inflow-angle bifurcation to 1.23 ± 0.12 dyne/cm^2 in the high inflow-angle bifurcation, while they increased from 0.004 ± 0.0005 dyne/cm^2 in the low inflow-angle sidewall to 0.029 ± 0.004 dyne/cm^2 in the high inflow-angle sidewall model (Fig. 4D). These results highlight a fundamental difference in the hemodynamics between sidewall and bifurcation aneurysms, in both the values of intraaneurysmal flow velocities, dome wall shear stress values, and their dependence on inflow angle. This angle is an important parameter describing the relationship of the aneurysm dome to its parent vessel, which was previously shown to be associated with rupture status in sidewall-type lesions and in this study not in bifurcation-type lesions.

TABLE 3: Results from multivariate logistic regression*

Group & Feature	OR	95% CI	p Value
BIF			
NSI	—	—	0.001†
SW			
H/W	7.97	2.35–32.3	<0.001†
SR	1.90	1.18–3.37	0.007†
IA	1.03	1.00–1.05	0.019†
combined			
H/W	2.69	1.37–5.51	0.004†
IA	1.01	1.00–1.03	0.008†
SR	1.33	1.07–1.68	0.009†

* Derived using forward stepwise regression, showing odds ratio (OR) per unit change for aneurysm rupture with 95% CIs. The odds ratio for NSI is not given, because it is limited between 0 and 1.
† Statistically significant.

Discussion

Role of Aneurysm Size

Authors of many clinical studies have argued for the primary role of larger aneurysm size in predicting rupture. Wiebers et al.[31] described the identification of a critical size of 10 mm, below which no aneurysm had ruptured. The ISUIA showed a near-zero rupture risk of 0.05% per year for aneurysms smaller than 10 mm in

Brought to you by Tufts University | Unauthenticated | Downloaded 11/04/25 02:25 PM UTC

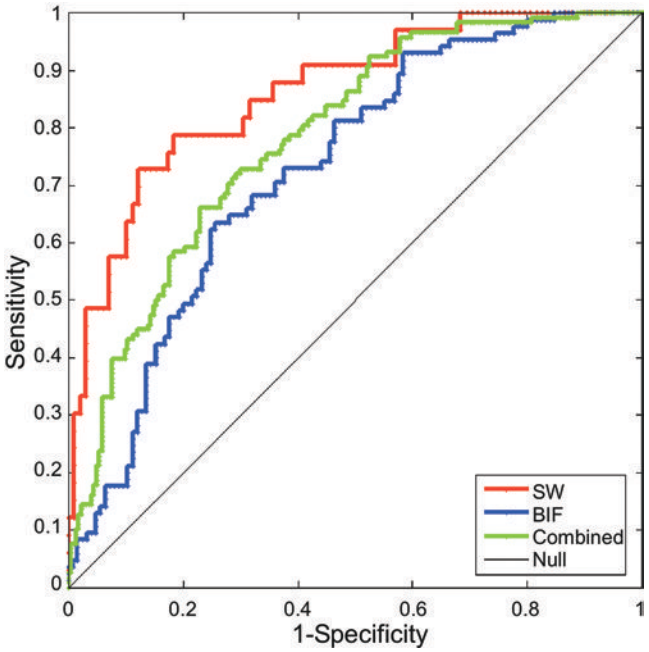


Fig. 3. Receiver-operating characteristic curves for multivariate logistic regression analysis of sidewall, bifurcation, and the combined aneurysm groups. The corresponding AUC values are 0.87 for the sidewall type, 0.67 for the bifurcation type, and 0.76 for the combined group.

diameter.[13,30] Our experience, however, similar to that of others,[3,8,36] has been that the majority of ruptured aneurysms are in fact smaller than 10 mm in diameter. Indeed, although our data are retrospective, they show that the mean aneurysm size is greater for ruptured aneurysms (7.76 mm, 95% CI 7.12–8.39 mm vs 6.45 mm, 95% CI 5.96–6.94 mm) in the overall combined group; however, the mean size for ruptured lesions is still well below the suggested critical size of 10 mm.

Furthermore, by analyzing sidewall and bifurcation aneurysms separately in a retrospective manner, we showed that aneurysm size does not differ significantly between ruptured and unruptured bifurcation aneurysms (6.96 mm, 95% CI 6.23–7.68 mm vs 6.79 mm, 95% CI 6.07–7.51 mm), with 39 ruptured aneurysms (58.2%) being smaller than 7 mm and 18 (26.8%) smaller than 5 mm. While it remains debatable that aneurysms might shrink after rupture,[16,32,36] the size difference between the suggested threshold of 10 mm and ruptured aneurysms smaller than 5 mm cannot be explained by this theoretical concern alone. Moreover, even within the sidewall subset, in which size proved to be correlated with rupture, 23 (67.6%) of the ruptured aneurysms were smaller than 10 mm and 8 (23.5%) were smaller than 7 mm. Although this study is, to the best of our knowledge, the first to include separate analyses of sidewall and bifurcation subtypes, some recent studies[23] (Lin N, Ho A, Gross BA, et al., abstract presented at the Congress of Neurological Surgeons Annual Meeting, 2010) on isolated middle cerebral artery aneurysms reported that aneurysm size was not statistically significant in discriminating rupture status of these lesions. In our data set, this is true within specific locations and in the overall bifurcation group.

Two other measures of size—aneurysm dome height and aneurysm volume—were also compared retrospectively, and this comparison confirmed that aneurysm size parameters did not differ significantly between ruptured and unruptured bifurcation aneurysms. In contrast, ruptured aneurysms in the sidewall group had significantly greater height and volume than unruptured aneurysms (data not shown). Our results also showed that the height of the aneurysm performed much better than maximum dome size (D_{max}) in all 3 groups studied and is, in fact, one of the best discriminant features for retrospective rupture status classification in sidewall aneurysms (AUC = 0.81). This dichotomy for aneurysm size between sidewall and bifurcation aneurysms may have clinical implications, given that aneurysm size remains the most commonly used clinical metric in analyzing rupture risk and is used daily to guide treatment decisions. Our results indicate that although this approach may be valid for sidewall aneurysms, it could be potentially misleading for predicting rupture differences in bifurcation aneurysms.

The disparate relevance of aneurysm size in sidewall- and bifurcation-type aneurysms uncovered in our study could shed light on the variability of the importance accorded to aneurysm size in different reports in the literature. For instance, we compared aneurysm location to aneurysm size and rupture risk reported by the ISUIA investigators.[13] The data set description suggests that a relative large percentage (54%) of low-risk (size < 10 mm) unruptured aneurysms in ISUIA were sidewall lesions. Similarly, in the data set described by Wiebers et al.,[32] 67% of aneurysms were reportedly sidewall type. This leads us to believe that data pointing to aneurysm size differentiating rupture status of aneurysms may be due to a relatively higher proportion of sidewall-type aneurysms in the studied population. Because ruptured aneurysms in practice tend to be bifurcation type, real-life results may be inconsistent with findings of these large prospective studies.

The current data indicate that not merely maximum aneurysm diameter but, more importantly, its relationship with other variables, such as parent vessel size, aneurysm width, and inflow angle, may be critical when assessing rupture status or risk.

Sidewall and Bifurcation Aneurysm Type: A Dichotomy

Separate analyses of sidewall and bifurcation aneurysms revealed that the 2 aneurysm subgroups behave differently with respect to the performance of shape- and size-based parameters in identifying rupture status in a retrospective manner. This is true for all the parameters evaluated in this study: D_{max}, height, height/width ratio, size ratio, and inflow angle were not significant in the bifurcation group, but were all correlated to rupture in the sidewall group. Univariate analysis showed the nonsphericity index and aspect ratio to be the only parameters that had a statistically significant correlation with rupture status in both bifurcation and sidewall groups. These findings are further reinforced by the statistical interaction analysis between the sidewall versus bifurcation dichotomous variable and the morphological parameters studied here. Indeed, interaction parameters based

Brought to you by Tufts University | Unauthenticated | Downloaded 11/04/25 02:25 PM UTC

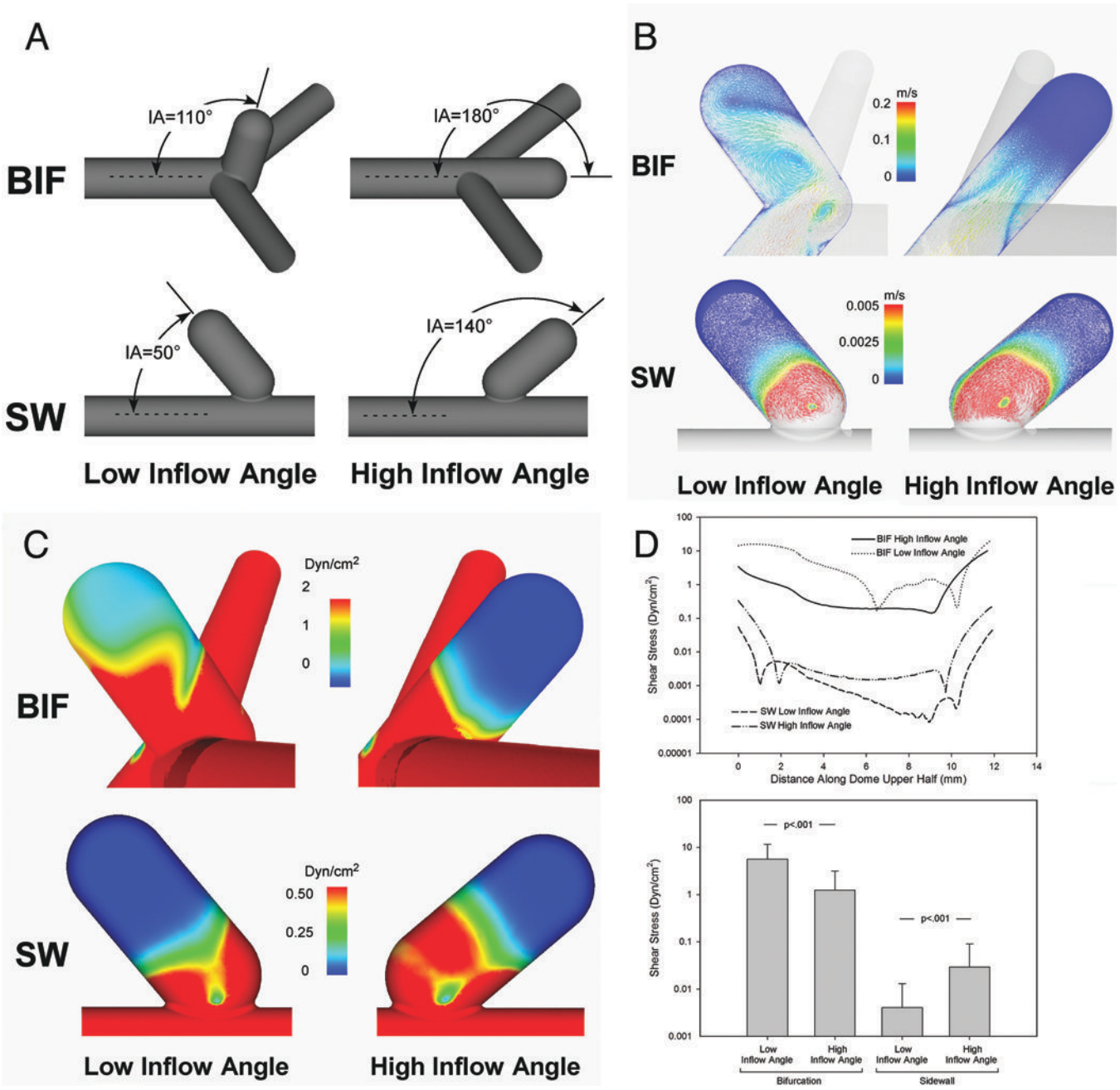


Fig. 4. **A:** Schematic of idealized bifurcation and sidewall aneurysms used in CFD analysis, showing a high and low inflow angle model for each class of aneurysm. **B:** Intraaneurysmal velocity magnitude and vectorial representation for bifurcation and sidewall models showing increasing velocities with higher inflow angle in the sidewall model but the opposite effect in the bifurcation model. **C:** Wall shear stress distribution showing lower values for higher inflow angles in the bifurcation model and the opposite effect in the sidewall counterpart. **D:** Wall shear stress profile *(upper)* over distance along the upper half of the aneurysm dome in a midsagittal plane and mean wall shear stress values *(lower)* over the corresponding area.

on D_{max}, height, height/width ratio, inflow angle, and size ratio were statistically significant discriminators of rupture status in the combined group. As expected, the interaction parameters of the sidewall versus bifurcation dichotomous variable with aspect ratio and nonsphericity index, the only parameters significant in both bifurcation and sidewall groups, were not statistically significant discriminators of rupture status in the combined group.

The morphological difference between sidewall and bifurcation lesions was also analyzed in the subgroup of 49 PCoA aneurysms, which present as either sidewall- or bifurcation-type depending on the size of the PCoA. While this PCoA subset population is small, the fact that D_{max}, height, height/width ratio, and size ratio were not significantly different between ruptured and unruptured aneurysms in the PCoA bifurcation lesions, reinforces

Brought to you by Tufts University | Unauthenticated | Downloaded 11/04/25 02:25 PM UTC

our findings that there are some inherent morphological factors that differentiate sidewall and bifurcation aneurysms even within the same location (PCoA in this case). Although this study involved a large aneurysm data set, the number of lesions in specific aneurysm locations is still too small for detailed statistical analysis. The size of acquired aneurysm data sets is growing, however, and future research will focus on location-specific morphological and hemodynamic analysis.

Computational fluid dynamics analysis on the effect of inflow-angle change in sidewall- and bifurcation-type aneurysms showed striking differences; while increasing inflow angle in the sidewall models showed an increase in flow, wall shear stress, and flow velocity inside the aneurysm dome, the opposite was true in the bifurcation models. In bifurcation lesions, an increase in inflow angle caused all of the mentioned parameters to decrease. Furthermore, wall shear stress in the upper half of the aneurysm dome was shown to be higher in both bifurcation models (high and low inflow angle) than in the sidewall model. All these observations stress the (hemodynamic) dichotomy between sidewall- and bifurcation-type aneurysms.

These observations lead us to hypothesize that sidewall aneurysms vary more than bifurcation aneurysms in terms of their dome morphology in relation to the parent vessel. This is highlighted by the fact that both inflow angle and size ratio were shown to be independently associated with rupture status in sidewall lesions. Both these parameters reflect aneurysm morphology in relation to the parent vessel. As for height/width ratio, which was also independently associated with rupture status in sidewall lesions, one can hypothesize that an increasing inflow angle could cause a greater inflow jet into the aneurysm dome, which has been shown to cause the aneurysm to grow preferentially in that direction.[9] This would lead to an increase in aneurysm height relative to width, in turn leading to a higher height/width ratio. Indeed, multivariate analysis identified inflow angle and height/width ratio, together with size ratio, as independently significant for discriminators of rupture status (AUC = 0.87).

Aneurysms that arise at bifurcations, however, seem to be less variable in these features; thus, rupture prediction in this group appears to be more challenging. Most size-related features (D_{max}, height, height/width ratio, and size ratio) failed to discriminate rupture status in bifurcation aneurysms. Indeed, in multivariate analysis only nonsphericity index, a measure of how nonspherical the aneurysm is, was identified as correlating with rupture status, but with an overall performance that was disappointing (AUC = 0.67). This finding could mean that aneurysm dome shape is more important for bifurcation lesions and that possibly bleb or daughter aneurysm formation could be more dangerous in these aneurysms. In the current database, which comprises 271 consecutive aneurysms, representing one of the largest such analyses to date, bifurcation aneurysms represent half of all aneurysms. More importantly, ruptured bifurcation aneurysms represent 66.3% of all ruptured aneurysms. Yet, despite the large sample size, shape and size parameters failed to discriminate rupture status in the bifurcation group. Although this study is retrospective in nature, it suggests that more research and new approaches may be needed to evaluate rupture risk prediction for this particular type of aneurysm.

This study revealed a significant difference in the discriminant performance between sidewall, bifurcation, and the combined group in both univariate and multivariate analyses. All evaluated features performed significantly better in the sidewall subset than in the bifurcation subset, with the combined group in an intermediate position.

Computational Fluid Dynamic Considerations

In this work, CFD analysis was performed as an additional tool to support the main morphological findings of the study. The major characteristics and differences between sidewall and bifurcation aneurysms—that is, the general geometrical relationship between lateral (sidewall) or terminal (bifurcation) aneurysms and their adjacent vessels—are captured in 2 generic aneurysm models. The preliminary results suggest that there may be significant hemodynamic differences between the 2 aneurysm types.

Computational fluid dynamics analysis has some limitations, as analyses of patient-related data are numerically intensive with results prone to variability related to technical details such as computational mesh density, convergence criteria, and fluid velocity boundary conditions that, among others, are not readily obtainable in clinical practice. Additionally, the interpretation of CFD analysis is often controversial. In a recent study, Xiang et al.[35] found that lower wall shear stress magnitudes and larger areas of low wall shear stress were related to aneurysm rupture. In another recent publication, Cebral et al.[5] reported that areas of low wall shear stress and measures of abnormally low shear forces on the aneurysm dome were not significantly different between ruptured and unruptured aneurysms. Instead, elevated values of maximum wall shear stress were reportedly associated with aneurysm rupture. In light of these controversial findings, in this study, we used CFD analysis as qualitative support for the main morphological analysis, rather than using quantitative parameters describing rupture status. However, given the dichotomy proposed here, it is very likely that such controversial findings regarding fluid dynamic interpretations have to do precisely with the fact that sidewall and bifurcation aneurysms are inherently different from a hemodynamic point of view; so depending on the sidewall/bifurcation distribution in a particular study, different results could be reported. Detailed hemodynamic analysis of multiple sidewall/bifurcation aneurysms based on patient angiographic data will be the focus of future work. Nonetheless, one must keep in mind that it has not been demonstrated that wall shear stress, whether high or low, is the critical causative factor in precipitating aneurysm rupture. This is especially important in light of the fact that most CFD simulations used for separating ruptured and unruptured aneurysms have assumed rigid walls, while the rupture phenomenon itself is thought to involve a weak potentially pulsatile wall segment.

Brought to you by Tufts University | Unauthenticated | Downloaded 11/04/25 02:25 PM UTC

Study Limitations

Analysis of aneurysm shape to identify aneurysm rupture status discriminants is based on the hypothesis that aneurysm shape does not change after rupture. Were shape to dramatically change after rupture, the current class of analysis would not be helpful. Even though evidence indicates that such a change does not occur,[1,21] consistent with intraoperative findings, conclusive data on this subject remain to be presented.

Furthermore, our analysis is retrospective and thus can only imply prediction of previously determined ruptured status. Our findings require validation in prospective randomized studies before they can be applied in risk assessment of incidentally found unruptured aneurysms in clinical practice. Although selection bias associated with the retrospective nature of this study may be a concern, the decision process for treatment versus observation in the ISUIA was also based on clinical grounds.

Finally, even though the current study describes one of the largest data sets acquired using 3D measuring techniques and highest resolution 3D rotational angiography, additional data from larger multicenter studies should be pooled and analyzed both retrospectively and prospectively to minimize the inherent bias and distribution imbalance that has characterized previous work.

Conclusions

The current study has uncovered a clear morphological and hemodynamic dichotomy between sidewall and bifurcation aneurysms, which were seen to behave differently under identical 3D shape-based analysis. Aneurysm size measurements did not distinguish between ruptured and unruptured bifurcation aneurysms even in univariate analysis. Although this study is retrospective in character and no evidence of future rupture prediction can be drawn for that reason, this finding should raise caution with respect to the sole use of size-based aneurysm characteristics as clinical risk-assessment tools in cerebral aneurysms. Conversely, the univariate prediction performance of all size and morphometric measures, such as D_{max}, height, aspect ratio, height/width ratio, size ratio, and inflow angle, was greater in the sidewall group than in the overall group, raising concern for bias toward these measures in previous analyses characterized by a sidewall aneurysm preponderance. Our results point toward a need for more sophisticated assessment tools than aneurysm size alone, as well as classification by aneurysm type in future prospective studies.

Disclosure

This work was supported by NIH-R21HL102685. Dr. Malek reports having received research support from Codman Neurovascular Inc., and Boston Scientific Corp., unrelated to the current study.

Author contributions to the study and manuscript preparation include the following. Conception and design: Malek, Baharoglu. Acquisition of data: all authors. Analysis and interpretation of data: Malek, Baharoglu, Lauric. Drafting the article: Malek, Baharoglu. Critically revising the article: all authors. Reviewed submitted version of manuscript: all authors. Approved the final version of the manuscript on behalf of all authors: Malek. Statistical analysis: Malek, Baharoglu, Lauric. Study supervision: Malek.

Acknowledgment

The authors would like to thank Courtney Petersen, P.A., for her assistance.

References

1. Asari S, Ohmoto T: Natural history and risk factors of unruptured cerebral aneurysms. **Clin Neurol Neurosurg 95:**205–214, 1993
2. Baharoglu MI, Schirmer CM, Hoit DA, Gao BL, Malek AM: Aneurysm inflow-angle as a discriminant for rupture in sidewall cerebral aneurysms: morphometric and computational fluid dynamic analysis. **Stroke 41:**1423–1430, 2010
3. Beck J, Rohde S, Berkefeld J, Seifert V, Raabe A: Size and location of ruptured and unruptured intracranial aneurysms measured by 3-dimensional rotational angiography. **Surg Neurol 65:**18–27, 2006
4. Broderick JP, Brott TG, Duldner JE, Tomsick T, Leach A: Initial and recurrent bleeding are the major causes of death following subarachnoid hemorrhage. **Stroke 25:**1342–1347, 1994
5. Cebral JR, Mut F, Weir J, Putman C: Quantitative characterization of the hemodynamic environment in ruptured and unruptured brain aneurysms. **AJNR Am J Neuroradiol 32:** 145–151, 2011
6. Dhar S, Tremmel M, Mocco J, Kim M, Yamamoto J, Siddiqui AH, et al: Morphology parameters for intracranial aneurysm rupture risk assessment. **Neurosurgery 63:**185–197, 2008
7. Fogelholm R, Hernesniemi J, Vapalahti M: Impact of early surgery on outcome after aneurysmal subarachnoid hemorrhage. A population-based study. **Stroke 24:**1649–1654, 1993
8. Forget TR Jr, Benitez R, Veznedaroglu E, Sharan A, Mitchell W, Silva M, et al: A review of size and location of ruptured intracranial aneurysms. **Neurosurgery 49:**1322–1326, 2001
9. Foutrakis GN, Yonas H, Sclabassi RJ: Saccular aneurysm formation in curved and bifurcating arteries. **AJNR Am J Neuroradiol 20:**1309–1317, 1999
10. Griffith TM, Edwards DH: Basal EDRF activity helps to keep the geometrical configuration of arterial bifurcations close to the Murray optimum. **J Theor Biol 146:**545–573, 1990
11. Hassan T, Timofeev EV, Saito T, Shimizu H, Ezura M, Matsumoto Y, et al: A proposed parent vessel geometry-based categorization of saccular intracranial aneurysms: computational flow dynamics analysis of the risk factors for lesion rupture. **J Neurosurg 103:**662–680, 2005
12. Hoh BL, Sistrom CL, Firment CS, Fautheree GL, Velat GJ, Whiting JH, et al: Bottleneck factor and height-width ratio: association with ruptured aneurysms in patients with multiple cerebral aneurysms. **Neurosurgery 61:**716–723, 2007
13. International Study of Unruptured Intracranial Aneurysms Investigators: Unruptured intracranial aneurysms—risk of rupture and risks of surgical intervention. **N Engl J Med 339:** 1725–1733, 1998
14. Juvela S, Porras M, Heiskanen O: Natural history of unruptured intracranial aneurysms: a long-term follow-up study. **J Neurosurg 79:**174–182, 1993
15. Juvela S, Porras M, Poussa K: Natural history of unruptured intracranial aneurysms: probability of and risk factors for aneurysm rupture. **J Neurosurg 93:**379–387, 2000
16. Kataoka K, Taneda M, Asai T, Yamada Y: Difference in nature of ruptured and unruptured cerebral aneurysms. **Lancet 355:**203, 2000 (Letter)
17. Kupersmith MJ, Hurst R, Berenstein A, Choi IS, Jafar J, Ransohoff J: The benign course of cavernous carotid artery aneurysms. **J Neurosurg 77:**690–693, 1992

Brought to you by Tufts University | Unauthenticated | Downloaded 11/04/25 02:25 PM UTC

18. Lanzer P, Topol EJ (eds): **PanVascular Medicine: Integrated Clinical Management.** Berlin: Springer-Verlag, 2002
19. Prestigiacomo CJ, He W, Catrambone J, Chung S, Kasper L, Pasupuleti L, et al: Predicting aneurysm rupture probabilities through the application of a computed tomography angiography–derived binary logistic regression model. Clinical article. **J Neurosurg 110:**1–6, 2009
20. Raghavan ML, Ma B, Harbaugh RE: Quantified aneurysm shape and rupture risk. **J Neurosurg 102:**355–362, 2005
21. Rahman M, Ogilvy CS, Zipfel GJ, Derdeyn CP, Siddiqui AH, Bulsara KR, et al: Unruptured cerebral aneurysms do not shrink when they rupture: multicenter collaborative aneurysm study group. **Neurosurgery 68:**155–161, 2011
22. Rahman M, Smietana J, Hauck E, Hoh B, Hopkins N, Siddiqui A, et al: Size ratio correlates with intracranial aneurysm rupture status: a prospective study. **Stroke 41:**916–920, 2010
23. Sadatomo T, Yuki K, Migita K, Taniguchi E, Kodama Y, Kurisu K: Morphological differences between ruptured and unruptured cases in middle cerebral artery aneurysms. **Neurosurgery 62:**602–609, 2008
24. Ujiie H, Tachibana H, Hiramatsu O, Hazel AL, Matsumoto T, Ogasawara Y, et al: Effects of size and shape (aspect ratio) on the hemodynamics of saccular aneurysms: a possible index for surgical treatment of intracranial aneurysms. **Neurosurgery 45:**119–130, 1999
25. Ujiie H, Tamano Y, Sasaki K, Hori T: Is the aspect ratio a reliable index for predicting the rupture of a saccular aneurysm? **Neurosurgery 48:**495–503, 2001
26. van Gijn J, Kerr RS, Rinkel GJE: Subarachnoid haemorrhage. **Lancet 369:**306–318, 2007
27. Vernooij MW, Ikram MA, Tanghe HL, Vincent AJ, Hofman A, Krestin GP, et al: Incidental findings on brain MRI in the general population. **N Engl J Med 357:**1821–1828, 2007
28. Wardlaw JM, White PM: The detection and management of unruptured intracranial aneurysms. **Brain 123:**205–221, 2000
29. Wiebers DO: Patients with small, asymptomatic, unruptured intracranial aneurysms and no history of subarachnoid hemorrhage should generally be treated conservatively: for. **Stroke 36:**408–409, 2005
30. Wiebers DO, Whisnant JP, Huston J III, Meissner I, Brown RD Jr, Piepgras DG, et al: Unruptured intracranial aneurysms: natural history, clinical outcome, and risks of surgical and endovascular treatment. **Lancet 362:**103–110, 2003
31. Wiebers DO, Whisnant JP, O'Fallon WM: The natural history of unruptured intracranial aneurysms. **N Engl J Med 304:** 696–698, 1981
32. Wiebers DO, Whisnant JP, Sundt TM Jr, O'Fallon WM: The significance of unruptured intracranial saccular aneurysms. **J Neurosurg 66:**23–29, 1987
33. Winn HR, Almaani WS, Berga SL, Jane JA, Richardson AE: The long-term outcome in patients with multiple aneurysms. Incidence of late hemorrhage and implications for treatment of incidental aneurysms. **J Neurosurg 59:**642–651, 1983
34. Womersley JR: Method for the calculation of velocity, rate of flow and viscous drag in arteries when the pressure gradient is known. **J Physiol 127:**553–563, 1955
35. Xiang J, Natarajan SK, Tremmel M, Ma D, Mocco J, Hopkins LN, et al: Hemodynamic-morphologic discriminants for intracranial aneurysm rupture. **Stroke 42:**144–152, 2011
36. Yasui N, Magarisawa S, Suzuki A, Nishimura H, Okudera T, Abe T: Subarachnoid hemorrhage caused by previously diagnosed, previously unruptured intracranial aneurysms: a retrospective analysis of 25 cases. **Neurosurgery 39:**1096–1101, 1996

Manuscript submitted February 23, 2011.
Accepted November 8, 2011.
Please include this information when citing this paper: published online January 13, 2012; DOI: 10.3171/2011.11.JNS11311.

Address correspondence to: Adel M. Malek, M.D., Ph.D., Department of Neurosurgery, Tufts Medical Center, 800 Washington Street, Boston, Massachusetts 02111. email: amalek@tuftsmedicalcenter.org.

Brought to you by Tufts University | Unauthenticated | Downloaded 11/04/25 02:25 PM UTC